

# RSC Advances



This is an *Accepted Manuscript*, which has been through the Royal Society of Chemistry peer review process and has been accepted for publication.

*Accepted Manuscripts* are published online shortly after acceptance, before technical editing, formatting and proof reading. Using this free service, authors can make their results available to the community, in citable form, before we publish the edited article. This *Accepted Manuscript* will be replaced by the edited, formatted and paginated article as soon as this is available.

You can find more information about *Accepted Manuscripts* in the [Information for Authors](#).

Please note that technical editing may introduce minor changes to the text and/or graphics, which may alter content. The journal's standard [Terms & Conditions](#) and the [Ethical guidelines](#) still apply. In no event shall the Royal Society of Chemistry be held responsible for any errors or omissions in this *Accepted Manuscript* or any consequences arising from the use of any information it contains.

# Effect of two-color laser pulse intensity ratio on intense terahertz generation

Chenhui Lu<sup>1,2)</sup>, Shian Zhang<sup>1,#)</sup>, Yunhua Yao<sup>1)</sup>, Shuwu Xu<sup>1,3)</sup>, Tianqing Jia<sup>1)</sup>, Jingxin Ding<sup>1)</sup>, and Zhenrong Sun<sup>1,\*)</sup>

<sup>1</sup>*State Key Laboratory of Precision Spectroscopy, and Department of Physics, East China*

*Normal University, Shanghai 200062, People's Republic of China*

<sup>2</sup>*College of Mechanical Engineering, Shanghai University of Engineering Science, Shanghai*

*201620, People's Republic of China*

<sup>3</sup>*School of Science, Nantong University, Nantong 226007, People's Republic of China*

## Abstract

We theoretically demonstrate the effect of intensity ratio of the two-color laser field on the terahertz generation based on a transient photocurrent model. We show that the terahertz generation depends on the intensity ratio of the two-color laser field at a given total laser intensity, and the optimal intensity ratio for the maximum terahertz generation will decrease with the increase of the total laser intensity. We also show that the final ionization degree can be used to explain the optimal intensity ratio change at different laser intensities. Furthermore, we utilize the increasing rate of electron density and the electron drift velocity to illustrate the physical mechanism of the maximum terahertz radiation generation.

PACS numbers: 42.65.Re, 32.80.Fb, 52.50.Jm

---

# Email: [sazhang@phy.ecnu.edu.cn](mailto:sazhang@phy.ecnu.edu.cn)

\* Email: [zrsun@phy.ecnu.edu.cn](mailto:zrsun@phy.ecnu.edu.cn)

## 1. Introduction

Terahertz (THz) pulse has been widely applied to various related fields, such as noninvasive imaging [1, 2], optical communications [3, 4], molecular spectroscopy [5], high-speed optical signal processing [6], biological and medical imaging [7, 8], and non-destructive evaluation (NDE) [9]. For some specific applications, such as remote sensing [10], it is crucial to generate the intense THz radiation. Conventional THz sources were usually achieved by semiconductor photoconductive switches [11, 12] or optical rectification in nonlinear crystals [13], while the THz field intensity by the two schemes is relatively low and its spectral range is narrow. Recently, as an alternative approach, two-color laser field has been proposed to generate the intense and broadband THz pulse [14-16]. In this two-color scheme, a fundamental femtosecond laser field combining with its second harmonic field are focused in air to generate gaseous plasma, and an intense THz pulse can be irradiated in the forward direction. This intense THz generation created by the two-color laser field has attracted considerable attention in both its related application and physical mechanism [17-26].

Initially, this intense THz generation was understood as a four-wave mixing process, but it was soon found that the Kerr nonlinearity is too small to explain the high THz field intensity [27]. In addition, several experimental results confirmed that the THz intensity threshold was coincident with the ionization threshold of gas molecules, which indicated that the plasma formation plays an important role in the THz generation process [18, 27]. Recently, a transient photocurrent model proposed

by Kim *et al.* was used to elucidate such THz generation in the two-color laser field [15, 19], and has been studied in many experiments and theoretical simulations [15-28]. In this model, tunneling ionization and subsequent electron motion will form a directional current, which is responsible for the intense THz generation. The intensity ratio of the second harmonic field to the fundamental laser field is an important parameter to affect tunneling ionization and subsequent electron motion, and consequently the THz generation. In previous works, this intensity ratio was usually controlled by varying the fundamental laser field intensity (or second harmonic field intensity) while keeping the second harmonic field intensity (or fundamental laser field intensity) [19, 29-32]. However, in this paper we demonstrate the effect of the intensity ratio of the second harmonic field to the fundamental laser field at a given total laser intensity on the THz generation, that is to say, both the fundamental laser field and its second harmonic field are simultaneously varied while the total laser intensity keeps a constant, which is different from the previous studies. We utilize the transient photocurrent model to simulate the THz generation in the two-color laser field. It is shown that the THz amplitude depends on the intensity ratio of the two-color laser field at a given total laser intensity and reaches to its maximal value at an optimal intensity ratio, while the optimal intensity ratio will decrease as the total laser intensity increases. It is also shown that the final ionization degree can explain the optimal intensity ratio change at different laser intensities. Furthermore, the physical mechanism of the maximal THz generation is also discussed and analyzed on the basis of the increasing rate of the electron density and the electron

drift velocity.

## 2. Theoretical model

Our theoretical simulation is based on the transient photocurrent model [15, 16], and a two-color laser field with a superposition of the fundamental laser field and its second harmonic field is given by

$$E(t) = \exp(-2 \ln 2 t^2 / \tau^2) [E_1 \cos \omega_0 t + E_2 \cos(2\omega_0 t + \phi)], \quad (1)$$

where  $E_1$  and  $E_2$  are, respectively, the field amplitude of the fundamental laser field and its second harmonic field,  $\tau$  is the pulse duration,  $\omega_0$  is the central frequency of the fundamental laser field, and  $\phi$  is the relative phase between the fundamental laser field and its second harmonic field. When the intense two-color laser field is focused in air, the free electrons will be created due to the tunneling ionization. The ionization ratio can be calculated by static tunneling (ST) model [33, 34] or Ammosov-Delone-Krainov (ADK) model [35, 36]. Here, the well-known static tunneling model is employed [22, 30], and the ionization rate can be expressed by

$$W_{st} = \frac{\alpha_{ST}}{|\varepsilon(t)|} \exp\left[-\left(\frac{\beta_{ST}}{\varepsilon(t)}\right)\right], \quad (2)$$

where  $\varepsilon(t) = E(t) / \varepsilon_a$ ,  $\varepsilon_a$  is the electric field in atomic unit,  $\alpha_{ST} = 4\omega_a r_H^{5/2}$  and  $\beta_{ST} = (2/3)r_H^{3/2}$ .  $\omega_a$  is the atomic frequency unit with  $\omega_a = \kappa^2 m e^4 / \hbar^3 \approx 4.13 \times 10^{16} \text{ S}^{-1}$ ,  $r_H$  is the ionization potential of the gas molecule relative to hydrogen atom  $r_H = U_{ion} / U_{ion}^H$ . In our simulation, we use  $U_{ion} = 15.6 \text{ eV}$  (for  $\text{N}_2$  gas) and  $U_{ion}^H = 13.6 \text{ eV}$ . Given the ionization rate  $W_{st}$ , the increasing rate of the electron density can be expressed by

$$\frac{dN_e(t)}{dt} = W_{st} [N_g - N_e(t)], \quad (3)$$

where  $N_e(t)$  is the time-dependent electron density and  $N_g$  is the initial neutral gas density. Thus, the final ionization degree  $W_{fi}$  after the laser pulse can be written as [23]

$$W_{fi} = N_e(t = \infty) / N_g. \quad (4)$$

Here,  $W_{fi}$  also can represent the final electron density after the passage of laser pulse. Once ionized, the electron will oscillate with the laser field, and the electron velocity at a subsequent time can be written as

$$v(t, t') = -\frac{e}{m} \int_{t'}^t dt'' E(t''), \quad (5)$$

where  $t'$  is the time when the electron is born. The initial velocity of the electron is assumed to be zero. Considering the contribution of all ionized electrons, the transverse electron current can be expressed by

$$J(t) = \int_{t_0}^t ev(t, t') \exp[-(t-t')/\gamma] dN_e(t'), \quad (6)$$

where  $dN_e(t')$  represents the change of electron density in the interval between  $t$  and  $t'$ ,  $v(t, t')$  is the velocity of these electron at time  $t$ , and  $\gamma$  is the phenomenological electron-ion collision rate ( $\gamma \cong 5 \text{ ps}^{-1}$  at atmospheric pressure) [22]. The time evolving electron current  $J(t)$  can generate electromagnetic pulse at THz frequency, and the THz field is proportional to the derivate of electron current  $J(t)$  and written as

$$E_{THz}(t) = \frac{d}{dt}[J(t)]. \quad (7)$$

Finally, the THz radiation spectrum is obtained by the Fourier transform of  $E_{THz}(t)$ , i.e.  $E_{THz}(\omega) = FFT[E_{THz}(t)]$ . In our simulation, the central frequency of the fundamental laser field is set to be  $\omega_0 = 12500 \text{ cm}^{-1}$ , and the pulse duration is  $\tau = 50$  fs.  $I_\omega$  and  $I_{2\omega}$  respectively represent the laser intensity of the fundamental laser field and its second harmonic field,  $I_{total}$  represents the total laser intensity of the two-color laser field, and  $R_I = I_{2\omega}/I_\omega$  is the intensity ratio of the two laser fields.

### 3. Results and discussion

Figure 1 shows the time-dependent electron current  $J(t)$  calculated from Eq. (6) (a) and its corresponding THz radiation spectrum  $E_{THz}(\omega)$  (b) with the relative phase of  $\phi = 0.5\pi$ , the relative intensity ratio of  $R_I = 0.2$  and the total laser intensity of  $I_{total} = 180 \text{ TW/cm}^2$ . As can be seen, the electron current  $J(t)$  is asymmetric distribution and a quasi-DC current arises after the laser pulse (see Fig. 1(a)). This current surge occurs in the time scale of photoionization process ( $< 100$  fs in the general case), which leads to the generation of electromagnetic radiation at THz frequencies (see Fig. 1(b)). The electromagnetic radiation spectrum also contains the fundamental laser field, its second harmonic field and their mixing fields, but here only the components at THz frequencies are our concern. As shown in Fig. 1(b), the THz spectrum has a wide range up to  $\sim 50$  THz, and the maximal value is at about  $\omega = 6$  THz.

In our work, we focus on the effect of the intensity ratio  $R_I$  of the two-color laser field on the THz generation at a given total laser intensity. Figure 2 shows the contour plot of THz amplitude as a function of the intensity ratio  $R_I$  and the relative

phase  $\phi$  with the total laser intensities of  $I_{total}=120$  (a), 180 (b), and 360 TW/cm<sup>2</sup> (c). It can be seen that the THz radiation is maximally obtained with the relative phase of  $\phi=\pi/2$  at all total laser intensities, and this result is the same as previous studies [15-17, 19]. However, the THz radiation is maximally obtained at different intensity ratios for different laser intensities. As shown in Fig. 2, the THz amplitude reaches the maximum value at the intensity ratios of  $R_I=1$ , 0.8 and 0.35 for the total laser intensities of  $I_{total}=120$ , 180 and 360 TW/cm<sup>2</sup>, respectively. That is to say, the optimal intensity ratio decreases with the increase of the total laser intensity.

Generally, the field amplitude of THz pulse relies on the ionization rate of gas molecules when the electric field of the two-color laser pulse is given [37]. Therefore, next we demonstrate the effect of the relative intensity ratio  $R_I$  and the total laser intensity  $I_{total}$  on the ionization rate. Figure 3 shows the final ionization degree  $W_{fi}$  as the function of the intensity ratio  $R_I$  with the total laser intensities of  $I_{total}=120$  (squares), 180 (circles) and 360 TW/cm<sup>2</sup> (triangles). As can be seen, the final ionization degree  $W_{fi}$  increases with the increase of the total laser intensity and almost reaches saturation at the total laser intensity of  $I_{total}=360$  TW/cm<sup>2</sup>. Furthermore, the final ionization degree  $W_{fi}$  shows a fast increase and then slow decrease process with the increase of the intensity ratio  $R_I$ , and is close to the maximal value at the intensity ratios of  $R_I=1$ , 0.8 and 0.35 for the total laser intensities of  $I_{total}=120$ , 180 and 360 TW/cm<sup>2</sup>, respectively. It's noteworthy that the optimal intensity ratio for the maximal ionization degree is almost the same as that for the maximal THz amplitude, which further indicates that the THz generation is

correlated with the plasma density. Obviously, the final ionization degree can explain why the optimal intensity ratio for maximal THz generation decreases with the increase of the total laser intensity in Fig. 2.

In this two-color laser field, the free electron is produced through tunneling ionization and then accelerated by the laser field, which results in the formation of transient electron current. Furthermore, these electrons not only oscillate with the laser field but also drift in the transverse direction. As a result, some residual-current density (RCD) remains in the produced plasma when the laser pulse is passed. This residual-current density RCD is an initial impetus to the plasma polarization and the excitation of transverse dipole oscillations, and therefore determines the THz emission [38, 39]. The dependence of THz generation on residual-current density RCD has been demonstrated in many experimental and theoretical studies [23, 30, 38-40]. Similarly, our results in Fig. 2 can also be explained by analyzing the residual-current density RCD. Here, we rewrite the Eq. (5) as

$$v(t, t') = -\frac{e}{m} \left[ \int_{-\infty}^t dt'' E(t'') - \int_{-\infty}^{t'} dt'' E(t'') \right]. \quad (8)$$

The first term in Eq. (8) is the electron oscillation velocity at laser frequency, and is constant when the laser pulse is passed. Therefore, after the passage of the laser pulse (i.e.,  $t \rightarrow \infty$ ), the velocity of electron is only determined by the second term in Eq. (8), which is usually defined as drift velocity

$$v_d(t') = \frac{e}{m} \int_{-\infty}^{t'} dt'' E(t''). \quad (9)$$

where  $e$  and  $m$  are the electron charge and mass. It is noted that the drift velocity

and the vector potential of the laser pulse are related as  $\vec{v}_d = -\frac{e}{m}\vec{A}$  [19, 23, 25, 40].

So residual-current density RCD can be written as

$$j_{RCD} = -e \int_{-\infty}^{\infty} dj_{RCD}(t) dt = -e \int_{-\infty}^{\infty} \frac{dN_e(t)}{dt} v_d(t) dt. \quad (10)$$

The peak amplitude of THz pulse is proportional to residual-current density RCD  $j_{RCD}$ , and written as

$$E_{THz} \propto j_{RCD}. \quad (11)$$

As shown in Eq. (11), the THz amplitude depends on the drift velocity  $v_d(t)$  and the increasing rate of electron density  $dN_e(t)/dt$ , and therefore this simple model can be used to explore the physical mechanism of the THz amplitude modulation in Fig. 2.

Since the THz amplitude depends on the intensity ratio of the two-color laser field, we discuss the THz generation by analyzing the drift velocity  $v_d(t)$  and the increasing rate of the electron density  $dN_e(t)/dt$  at the optimal intensity ratio and it's both sides. Figure 4(a) shows the field amplitude of the two-color laser pulse in an half optical period with the intensity ratios of  $R_I=0.6$  (black dotted line), 1 (red solid line) and 1.4 (blue dashed line) for the total laser intensity of  $I_{total}=120$  TW/cm<sup>2</sup> and the relative phase of  $\phi=0.5\pi$ . As can be seen, the field amplitude increases with the increase of the intensity ratio  $R_I$ . As shown in Eq. (2), the ionization process only occurs near extreme of the electric field and the ionization rate  $W_{st}$  depends on the amplitude of electric field, and thus the stronger laser pulse will produce the more free electrons. Figure 4(b) shows the drift velocity  $v_d(t)$  and the increasing rate of electron density  $dN_e(t)/dt$  in the optical period for the three intensity ratios. One can see that the increasing rate of electron density  $dN_e(t)/dt$  shows the same

evolution behavior with the field amplitude in Fig. 4(a), which is consistent with our above prediction. However, the absolute value of drift velocity  $v_d(t)$  shows an opposite behavior, which decreases as the intensity ratio  $R_I$  increases, here the minus sign only indicate that direction of electron current. Since the THz amplitude depends on both the drift velocity  $v_d(t)$  and the increasing rate of the electron density  $dN_e(t)/dt$  (see Eq. (10) and Eq. (11)), the former decreases while the latter increases with the increase of the intensity ratio, and therefore there will be a maximal THz amplitude at an appropriate intensity ratio. Figure 4(c) shows the transition residual-current density RCD  $dj_{RCD}(t)$  at the three intensity ratios calculated from Fig. 4(b) based on Eq. (10). One can see that the transition residual-current density RCD  $dj_{RCD}(t)$  is maximally obtained at the intensity ratio of  $R_I=1$  (see inset of Fig. 4(c)). Since the transition residual-current density RCD  $dj_{RCD}(t)$  has the same behavior in each optical period at the three intensity ratios, the whole residual-current density RCD  $j_{RCD}$  is maximal value at the intensity ratio  $R_I=1$ , which can radiate the maximal THz emission. Consequently, one can conclude that the THz amplitude at the optimal intensity ratio benefits from lager electron density comparing with the lower intensity ratio, while benefits from lager drift velocity comparing with the higher intensity ratio.

In above analysis, the laser intensity is relatively low, and therefore only a part of gas molecules are ionized. As shown in Eq. (3), the increasing rate of the electron density is given by  $dN_e(t)/dt = W_{st} [N_g - N_e(t)]$ , where  $N_g - N_e(t)$  is density of neutral gas at time t. Since  $N_e(t)$  is rather small at low laser intensity, the increasing

rate of electron density can be further expressed by  $dN_e(t)/dt \approx W_{st}N_g$ , and thus its decrease in each optical period can be neglected. In this case, the electron current change in one optical period by varying the intensity ratio of the two-color laser field can directly reflect the whole electron current modulation. However, when the laser intensity is high enough, the gas molecules can be completely ionized in a few optical periods, above analysis method cannot be utilized, it need to consider the transition residual-current density RCD  $dj_{RCD}(t)$  in each optical period. Figure 5 shows the transition residual-current density RCD  $dj_{RCD}(t)$  in the range of the whole laser pulse duration with the total laser intensity of  $I_{total}=360 \text{ TW/cm}^2$  for the intensity ratios of  $R_I=0.1$  (black solid line), 0.35 (red dashed line) and 1.8 (blue dotted line). As can be seen, the gas molecules will be completely ionized within about fifteen optical periods in this high laser intensity. With the increase of the intensity ratio  $R_I$ , the transition residual-current density RCD  $dj_{RCD}(t)$  increases in the first optical few optical periods, while decreases in the last few optical periods, and thus the whole residual-current density RCD  $J_{RCD}$  is maximally obtained at a approximate intensity ratio. We also present the whole residual-current density RCD  $J_{RCD}$  by integrating the transition RCD  $dj_{RCD}(t)$  over the entire laser pulse for the three intensity ratios, as shown in inset of Fig. 5. As can be seen, the whole residual-current density RCD  $J_{RCD}$  obtains the maximal value at the intensity ratio of  $R_I=0.35$ , which results in the maximal THz radiation.

Finally, we present the dependence of the THz amplitude on the total laser intensity  $I_{total}$  at the optimal intensity ratio, as shown in Fig. 6. One can see that the

THz output first increases and then approaches to saturation with the increase of the total laser intensity  $I_{total}$ . Obviously, such intensity dependence is similar to the previous report [15, 17]. In previous studies, the intensity ratio is kept a constant, but here we present the THz amplitude at the optimal intensity ratio, and therefore it represents the maximally attainable THz output at each given laser intensity. The THz amplitude saturation in the high laser intensity can be attributed to the complete ionization in the gaseous molecules, as shown in Figs. 3 and 5.

#### 4. Conclusions

In conclusion, we have theoretically shown that the intensity ratio of the two-color laser field at a given total laser intensity will affect the THz generation. Our results showed that the optimal intensity ratio for the maximal THz generation decreases with the increase of the total laser intensity, and the final ionization degree can explain the optimal intensity ratio change at different laser intensities. Furthermore, the physical mechanisms of the maximal THz generation at low and high laser intensities were discussed and analyzed by considering the drift velocity and the increasing rate of the electron density. Our results will be very useful for further understanding the intense THz generation and its control, and are expected to be applied in various related fields.

#### Acknowledgements

This work was partly supported by National Natural Science Fund (Nos. 51132004 and 11474096) and Shanghai Municipal Science and Technology Commission (No.

14JC1401500).

## References

1. P. Y. Han, G. C. Cho, and X.-C. Zhang, "Time-domain transillumination of biological tissues with terahertz pulses," *Opt. Lett.* 25, 242 (2000).
2. J. L. Johnson, T. D. Dorney, and D. M. Mittleman, "Enhanced depth resolution in terahertz imaging using phase-shift interferometry," *Appl. Phys. Lett.* 78, 835 (2001).
3. T. Kleine-Ostmann and T. Nagatsuma, "A review on terahertz communications research," *J. Infrared. Milli. Terahertz Waves* 32(2), 143 (2011).
4. H. J. Song and T. Nagatsuma, "Present and future of terahertz communications," *IEEE. Tran. Terahertz Sci. Tech.* 1, 256 (2011).
5. E. Knoesel, M. Bonn, J. Shan, and T. F. Heinz, "Charge transport and carrier dynamics in liquids probed by THz time-domain spectroscopy," *Phys. Rev. Lett.* 86, 340 (2001).
6. D. S. Citrin, "Picosecond dynamics of terahertz-sideband generation in far-infrared illuminated quantum wells," *Appl. Phys. Lett.* 76, 3176 (2000).
7. D. D. Arnone, C. M. Ciesla, A. Corchia, S. Egusa, M. Pepper, J. M. Chamberlain, C. Bezzant, and E. H. Linfield, "Applications of terahertz (THz) technology to medical imaging," *Proc. SPIE* 3828, 209 (1999).
8. Z. D. Taylor, R. S. Singh, D. B. Bennett, P. Tewari, C. P. Kealey, N. Bajwa, M. O. Culjat, A. Stojadinovic, H. Lee, J.-P. Hubschman, E. R. Brown, and W. S. Grundfest. "THz medical imaging: in vivo hydration sensing," *IEEE. Trans. THZ Sci. Technol.* 1, 201 (2011).
9. J. B. Jackson, M. Mourou, J. F. Whitaker, I. N. Duling III, S. L. Williamson, M. Menu, and G. A. Mourou, "Terahertz imaging for non-destructive evaluation of mural paintings," *Opt.*

- Commun. 281, 527 (2008)
10. J. Liu, J. Dai, S. L. Chin, and X.-C. Zhang, "Broadband terahertz wave remote sensing using coherent manipulation of fluorescence from asymmetrically ionized gases," *Nat. Photonics* **4**, 627 (2010).
  11. D. H. Auston and P. R. Smith, "Generation and detection of millimeter waves by picosecond photoconductivity," *Appl. Phys. Lett.* **43**, 631 (1983).
  12. Ch. Fattinger and D. Grischkowsky, "Terahertz beams," *Appl. Phys. Lett.* **54**, 490 (1989).
  13. D. H. Auston, K. P. Cheung, J. A. Valdmanis, and D. A. Kleinman, "Cherenkov radiation from femtosecond optical pulses in electro-optic media," *Phys. Rev. Lett.* **53**, 1555 (1984).
  14. D. J. Cook and R. M. Hochstrasser, "Intense terahertz pulses by four-wave rectification in air," *Opt. Lett.* **25**, 1210 (2000).
  15. K. Y. Kim, J. H. Glowia, A. J. Taylor, and G. Rodriguez, "Terahertz emission from ultrafast ionizing air in symmetry-broken laser fields," *Opt. Express* **15**, 4577 (2007).
  16. T. I. Oh, Y. S. You, N. Jhajj, E. W. Rosenthal, H. M. Milchberg, and K. Y. Kim, "Intense terahertz generation in two-color laser filamentation: energy scaling with terawatt laser systems," *New J. Phys.* **15**, 75002 (2013).
  17. H. G. Roskos, M. D. Thomson, M. Kreß, and T. Löffler, "Broadband THz emission from gas plasmas induced by femtosecond optical pulses: From fundamentals to applications," *Laser Photonics Rev.* **1**, 349 (2007).
  18. N. Karpowicz, X. Lu, and X.-C. Zhang, "Terahertz gas photonics," *J. Mod. Optic.* **56** (10), 1137 (2009).
  19. K. Y. Kim, "Generation of coherent terahertz radiation in ultrafast laser-gas interactions),"

- Phys. Plasmas 16 (5), 56706 (2009).
20. I. Babushkin, W. Kuehn, C. Köhler, S. Skupin, L. Bergé, K. Reimann, M. Woerner, J. Herrmann, and T. Elsaesser, "Ultrafast spatiotemporal dynamics of terahertz generation by ionizing two-color femtosecond pulses in gases," *Phys. Rev. Lett.* 105 (5), 53903 (2010).
  21. H. Dai and J. Liu, "Phase dependence of the generation of terahertz waves from two-color laser-induced gas plasma," *J. Optics* 13 (5), 55201 (2011).
  22. I. Babushkin, S. Skupin, A. Husakou, C. Köhler, E. Cabrera-Granado, L. Bergé, and J. Herrmann, "Tailoring terahertz radiation by controlling tunnel photoionization events in gases," *New J. Phys.* 13 (12), 123029 (2011).
  23. H.-C. Wu, J. Meyer-ter-Vehn, and Z.-H. Sheng, "Phase-sensitive terahertz emission from gas targets irradiated by few-cycle laser pulses," *New J. Phys.* 10 (4), 43001 (2008).
  24. D. Zhang, Z. Lü, C. Meng, X. Du, Z. Zhou, Z. Zhao, and J. Yuan, "Synchronizing terahertz wave generation with attosecond bursts," *Phys. Rev. Lett.* 109 (24), 243002 (2012).
  25. J. Das and M. Yamaguchi, "Tunable narrow band THz wave generation from laser induced gas plasma," *Opt. Express* 18 (7), 7038 (2010).
  26. A. V. Borodin, N. A. Panov, O. G. Kosareva, V. A. Andreeva, M. N. Esaulkov, V. A. Makarov, A. P. Shkurinov, S. L. Chin, and X.-C. Zhang, "Transformation of terahertz spectra emitted from dual-frequency femtosecond pulse interaction in gases," *Opt. Lett.* 38 (11), 1906 (2013).
  27. M. Kress, T. Löffler, S. Eden, M. Thomson, and H. G. Roskos, "Terahertz-pulse generation by photoionization of air with laser pulses composed of both fundamental and second-harmonic waves," *Opt. Lett.* 29 (10), 1120 (2004).

28. K. Y. Kim, A. J. Taylor, J. H. Glowina, and G. Rodriguez, "Coherent control of terahertz supercontinuum generation in ultrafast laser–gas interactions," *Nat. photonics* 2 (10), 605 (2008).
29. X. Xie, J. Dai, and X. -C. Zhang, "Coherent control of THz wave generation in ambient air," *Phys. Rev. Lett.* 96, 075005 (2006).
30. N. V. Vvedenskii, A. I. Korytin, V. A. Kostin, A. A. Murzanev, A. A. Silaev and A. N. Stepanov, "Two-color laser-plasma generation of terahertz radiation using a frequency-tunable half harmonic of a femtosecond pulse," *Phys. Rev. Lett.* 112, 055004 (2014)
31. I. Babushkin, S. Skupin, and J. Herrmann, "Generation of terahertz radiation from ionizing two-color laser pulses in Ar filled metallic hollow waveguides", *Opt. Express* 18, 9658 (2010)
32. W. Zhang, S.-F. Guo, S.-Q. Duan, and X.-G. Zhao, "Terahertz wave generation from hyper-Raman lines in two-level quantum systems driven by two-color lasers", *Opt. Express* 21, 21349 (2013)
33. D. W. Schumacher and P. H. Bucksbaum, "Phase dependence of intense-field ionization," *Phys. Rev. A* 54 (5), 4271 (1996).
34. P. B. Corkum, N. H. Burnett, and F. Brunel, "Above-threshold ionization in the long-wavelength limit," *Phys. Rev. Lett.* 62, 1259 (1989).
35. P. B. Corkum, "Plasma perspective on strong field multiphoton ionization," *Phys. Rev. Lett.* 71 (13), 1994 (1993).
36. S. C. Rae and K. Burnett, "Detailed simulations of plasma-induced spectral blueshifting,"

- Phys. Rev. A 46 (2), 1084 (1992).
37. X. Sun and X. -C. Zhang, "Terahertz radiation in alkali vapor plasmas," *Appl. Phys. Lett.* 104, 191106 (2014)
  38. V. B. Gildenburge and N. V. Vvedenskii, "optical-to-THz wave conversion via excitation of plasma oscillations in the tunneling ionization process," *Phys. Rev. Lett.* 98, 245002 (2007)
  39. A. A. Silaev and N. V. Vvedenskii, "residual-current excitation in plasmas produced by few-cycle laser pulse, *Phys. Rev. Lett.* 102, 115005 (2009)
  40. C. S. Liu and V. K. Tripathi, "Tunable terahertz radiation from a tunnel ionized magnetized plasma cylinder," *J. Appl. Phys.* 105, 013313 (2009)

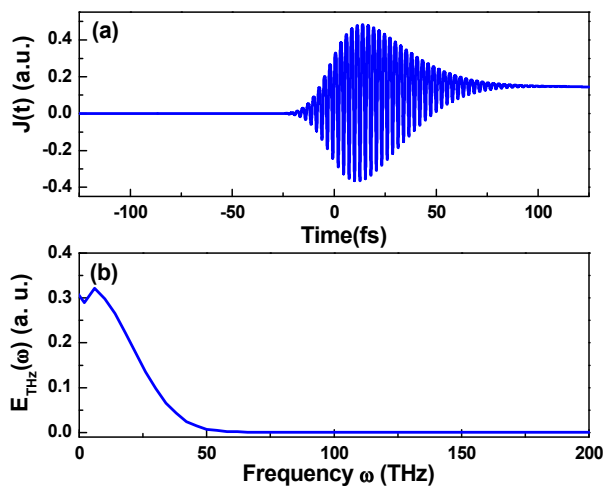


Figure 1 (Color online) Time-varying electron current  $J(t)$  (a) and its corresponding THz radiation spectrum  $E_{THz}(\omega)$  (b) with the relative phase of  $\phi = 0.5\pi$ , the relative intensity ratio of  $R_l = 0.2$  and the total laser intensity of  $I_{total} = 180 \text{ TW/cm}^2$ .

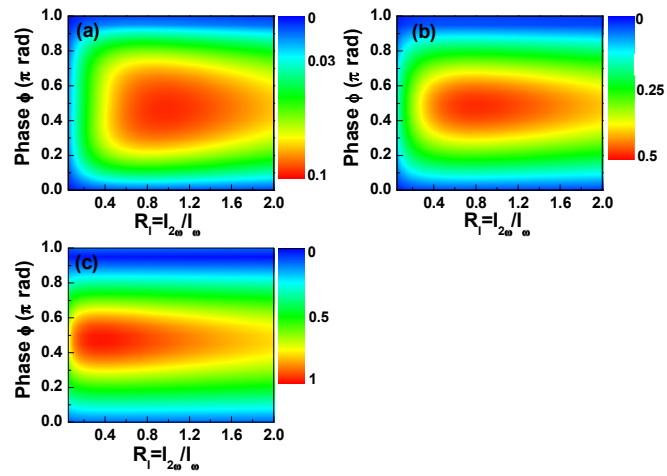


Figure 2 (Color online) Contour plot of the THz amplitude as a function of the intensity ratio  $R_1$  and the relative phase  $\phi$  with the total laser intensities of  $I_{total}=120$  (a), 180 (b) and 360  $\text{TW}/\text{cm}^2$  (c).

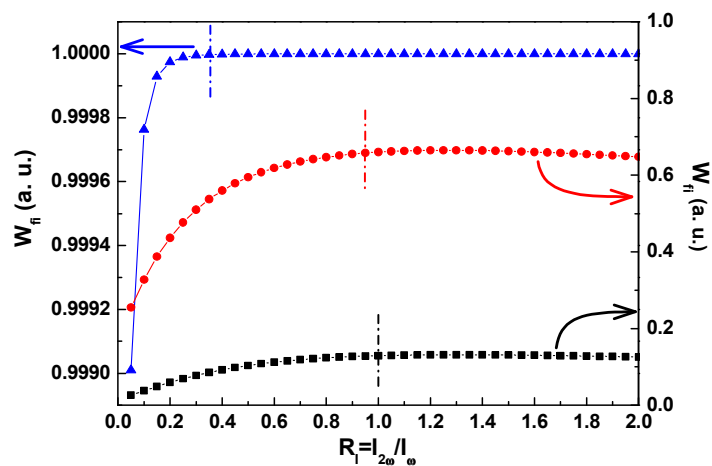


Figure 3 (Color online) The final ionization degree  $W_{fi}$  as a function of the intensity ratio  $R_l$  with the total laser intensities of  $I_{total}=120$  (black squares), 180 (red circles) and  $360 \text{ TW/cm}^2$  (blue triangles). The dashed lines are used to show the position of the optimal intensity ratio.

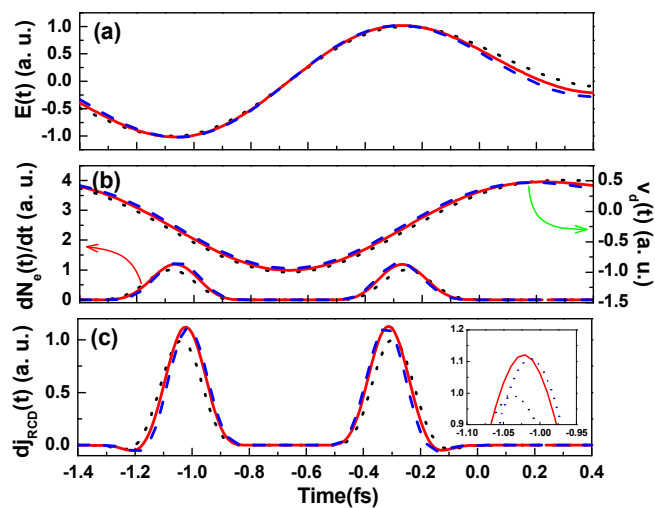


Figure 4 (Color online) The field amplitude of the two-color laser pulse (a), the electron drift velocity  $v_d(t)$  and the increasing rate of electron density  $dN_e(t)/dt$  (b), and the transition residual-current density RCD  $dj_{RCD}(t)$  (c) in an half optical period for the intensity ratios of  $R_I=0.6$  (black dotted line), 1 (red solid line) and 1.4 (blue dashed line). Inset in Fig. 4(c) shows the peak amplitude of  $dj_{RCD}(t)$  for the three intensity ratios.

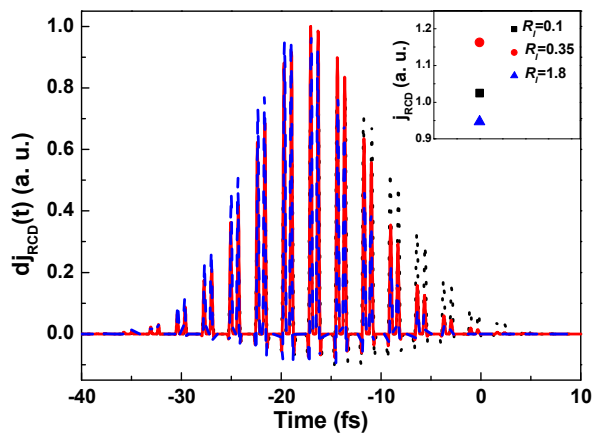


Figure 5 (Color online) The transition residual-current density RCD  $dj_{RCD}(t)$  in the whole laser pulse duration with the total laser intensity of  $I_{total}=360 \text{ TW/cm}^2$  for the intensity ratios of  $R_f = 0.1$  (black solid line),  $0.35$  (red dashed line) and  $1.8$  (blue dotted line). Inset shows the whole residual-current density RCD  $j_{RCD}$  for the three intensity ratios.

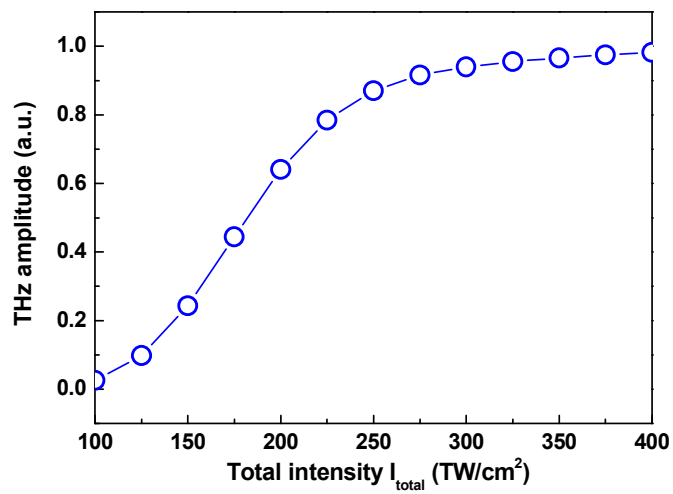


Figure 6 (Color online) The THz amplitude as a function of the total laser intensity  $I_{total}$  at the optimal intensity ratio.